DNA Nanostructures

DOI: 10.1002/anie.200704836

High-Throughput, Real-Time Monitoring of the Self-Assembly of DNA Nanostructures by FRET Spectroscopy**

Barbara Saccà, Rebecca Meyer, Udo Feldkamp, Hendrik Schroeder, and Christof M. Niemeyer**

Since its pioneering description in 1982 by Seeman,[1] DNA-based nanotechnology has undergone a rapid development, such that the self-assembly of synthetic oligonucleotides is nowadays almost routinely applied for the fabrication of superlattices with nanometer-scaled features.[2] Despite these advances, the characterization of the self-assembled nanostructures is still limited to only a few physicochemical methodologies, mainly, gel electrophoresis, atomic force microscopy (AFM) or, more recently, cryo-transmission electron microscopy (cryo-TEM).[2] All these methods are usually destructive and allow only for end-point analysis of the final product, thereby precluding the possibility to detect and optimize the assembly process through manipulation of the same sample. To overcome these obstacles, we report herein a novel method based on Förster resonance energy transfer (FRET) spectroscopy to monitor in real time and with high throughput the self-assembly of DNA tiles and nanoarrays.[3] As demonstrated for several DNA nanostructures of different sequence design, this approach allows the complete thermodynamic characterization of the assembly process.

As schematically illustrated in Figure 1 a, we chose a set of nine oligomers which self-assemble into a cross-shaped DNA motif, a 4 × 4 tile composed of four four-arm DNA branched junctions.[4] Five individual tiles, denoted A, A^2, B, B^2, and B^3 (Figure S1 a–e in the Supporting Information)[5] were designed bearing distinct differences in oligonucleotide composition. Tiles A^2 and B^3 were designed such that they associate specifically with each other to form a two-dimensional nanoscaled lattice (A^2B^3) with an internal periodicity of approximately 19.3 nm (Figure 2 a, and Figure S3 in the Supporting Information).

To enable the in situ monitoring of the self-assembly process by FRET spectroscopy, the two oligomers of the "east" arm of the tile (NE and SE) were labeled at terminal positions with fluorescein (Fsc) as the donor and tetramethylrhodamine (TAMRA) as the acceptor. The distance between the two fluorophores in the final superstructures (ca. 4–5 nm) and their relative positioning within all the various constructs allowed us to analyze the superstructures' formation and their thermodynamic properties.[6] The self-assembly of an equimolar mixture comprising all the oligomers necessary for a distinct superstructure (0.4 μM each) was then monitored online using a real-time PCR thermocycler.[5] The FRET efficiency was measured as the decrease of the Fsc donor emission owing to energy transfer to the TAMRA acceptor,[7] and its variation with temperature was monitored in the range between 29 and 80 °C (both heating and cooling rates were 0.1 °C min^{-1}). A typical example of the obtained assembly/disassembly curves is shown in Figure 1 b. The superimposition of the heating and cooling profiles, as well as the rapid variation of the assembled fraction (θ) in a relatively narrow temperature range around T_m, revealed reversibility and cooperativity of superstructure formation (Figure 1 b, and Figure S4 a–e in the Supporting Information). This result indicates that the process involves equilibrium between only two species, that is, the dissociated oligomers

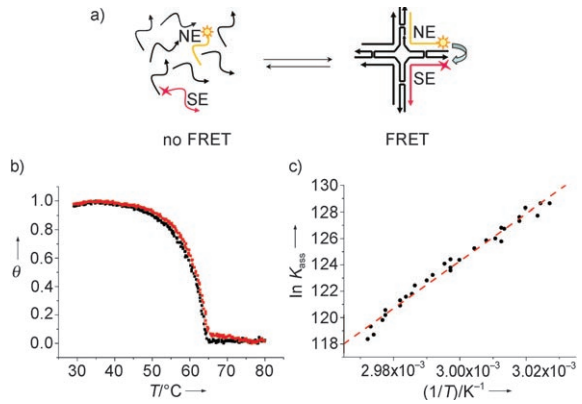

Figure 1. a) Labeling strategy used for the FRET thermal analysis of the self-assembly of individual DNA tiles. The 3′-Fsc-labeled NE (or BNE-3 for tile B^3) and the 5′-TAMRA-labeled SE (or BSE-3 for tile B^3) oligomers were chosen as reporter strands. The distance between the two fluorophores in the final structure was theoretically estimated to be about 4 nm, thus enabling an efficient energy transfer. b) FRET thermal analysis obtained for tile A (0.4 μM). Variation of the assembled fraction (θ) during heating (red curve) and cooling (black curve) of the oligomer mixture in the range 29–80 °C (0.1 °C min^{-1}). The transition is reversible and cooperative (T_m = 61.0 °C), indicating that the assembly/disassembly proceeds according to a simple two-state model. Application of the van't Hoff analysis leads to the Arrhenius plot shown in (c). The slope and the intercept of the linear regression (dashed red curve) yield, respectively, changes in enthalpy (ΔH_{VH}) and entropy (ΔS_{VH}) of the assembly process.

[*] Dr. B. Saccà, R. Meyer, Dr. U. Feldkamp, Dr. H. Schroeder, Prof. Dr. C. M. Niemeyer
Technische Universität Dortmund, Fakultät Chemie
Biologisch-Chemische Mikrostrukturtechnik
Otto-Hahn-Strasse 6, 44227 Dortmund (Germany)
Fax: (+49) 231-755-7082
E-mail: barbara.sacca@uni-dortmund.de
christof.niemeyer@uni-dortmund.de

[**] This work was supported by the Zentrum für Angewandte Chemische Genomik, a joint research initiative founded by the European Union and the Ministry of Innovation and Research of the state Northrhine Westfalia and the Deutsche Forschungsgemeinschaft (grant FE 943/1-1 to U.F.).

Supporting information for this article is available on the WWW under http://www.angewandte.org or from the author.

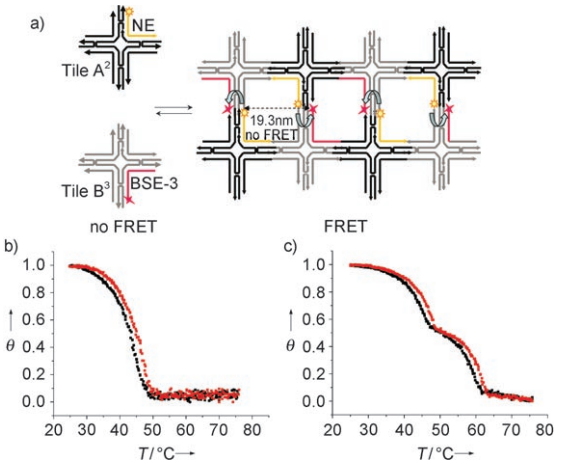

Figure 2. a) Two-tile labeling strategy adopted for the FRET thermal analysis of tile-to-tile association into the A^2B^3 superlattice. The reporter oligomers are the 5′-Fsc-labeled NE strand of tile A^2 and the 3′-TAMRA-labeled BSE-3 strand of tile B^3. Correct formation of the nanoarray leads to FRET between the fluorophores of adjacent tiles. b,c) FRET thermal curves obtained for the A^2B^3 nanoarray formation using the two-tile (b) or the single-tile labeling strategy (c). The overlap of the heating (red curve) and cooling profiles (black curve) revealed reversibility of the assembly/disassembly process. Note that with the two-tile labeling (depicted in Figure 2a) a single cooperative transition is visible ($T_m = 43.3\,°C$), which indicates tile-to-tile assembly. In contrast, the one-tile labeling enables observation of both tile A^2 formation ($T_m = 59.7\,°C$) and the tile-to-tile assembly ($T_m = 44.0\,°C$).

Table 1: van't Hoff thermodynamic parameters for the self-assembly of different DNA nanostructures.

DNA nanostructure[a]	T_m[b] [°C]	ΔH_{VH}[c] [kcal mol^{-1}]	ΔS_{VH}[c] [kcal mol^{-1} K^{-1}]	ΔG_{VH}[d] (25 °C) [kcal mol^{-1}]
A	61.0	-370 ± 10	-0.86 ± 0.03	-113 ± 1
A(nc)	45.8	-213 ± 5	-0.45 ± 0.025	-78 ± 7
A^2	59.9	-324 ± 34	-0.73 ± 0.1	-107 ± 4
B	61.4	-477 ± 10	-1.18 ± 0.03	-125 ± 1
B^2	61.2	-379 ± 31	-0.89 ± 0.09	-114 ± 4
B^3	63.1	-451 ± 22	-1.10 ± 0.06	-124 ± 3
$A^2B^3_{\text{tile-to-tile}}$	43.3	-113 ± 3	-0.33 ± 0.01	-16 ± 4
A^2B^3(nc)	n.a.[e]	n.a.	n.a.	n.a.

[a] The single tiles A, A^2, B, B^2, and B^3, as well as the assembled nanoarray A^2B^3, were all prepared at 0.4 μM concentration in 1X TEMg buffer, as described in the Supporting Information. The negative controls (nc) for tile A and nanoarray A^2B^3 were prepared similarly to the corresponding full superstructures while oligomer C and oligomers AN and BS-3 were omitted in A(nc) and A^2B^3(nc), respectively. The data reported for the A^2B^3 nanoarray formation refer to the tile-to-tile association step (see Figure 2b, and Figure S7a in the Supporting Information). [b] The melting temperature (T_m) is defined as the temperature at which 50% of the final structure is fully assembled and 50% is completely dissociated. [c] The van't Hoff enthalpy and entropy changes (ΔH_{VH} and ΔS_{VH}) for the reversible thermal transitions were calculated as described in the Supporting Information. [d] Free energies (ΔG_{VH}) were calculated at 25 °C using the Gibbs equation: $\Delta G_{VH} = \Delta H_{VH} - T\Delta S_{VH}$. [e] In the negative control for nanoarray formation, A^2B^3(nc), determination of the thermodynamic parameters was not applicable (n.a.).

and the fully assembled tile. Since we could experimentally exclude the formation of intermediate species (Table S2 and Figures S5, S6 in the Supporting Information), application of the van't Hoff analysis to the thermal curves (Figure 1c) was possible in order to calculate the thermodynamic profile of the nanostructure formation.[8]

The results obtained for the assembly of various different tiles are summarized in Table 1, and additional data obtained for varying concentrations are listed in Table S1 in the Supporting Information.[5] All constructs under investigation revealed largely negative values of ΔH_{VH}, indicating a favorable enthalpic contribution to the assembly process. This result can be attributed to the cooperative formation of extensive hydrogen bonding leading to the enthalpically favored final superstructure. On the other hand, the negative values of ΔS_{VH} indicate the predictable increase in internal order of the system resulting from the perfect matching of all the oligomers in the final construct. Nonetheless, the much higher enthalpic terms account for the stability of the superstructures under normal conditions, as indicated by the values of free energy at 25 °C (ΔG_{VH}). Control experiments in which the assembly of tile A was carried out in the absence of the central oligomer C revealed a significantly lowered thermal transition during the assembly/disassembly process (A(nc) in Table 1, and Figure S4f in the Supporting Information).

Tiles A, A^2, B, and B^2 (Figure S1a–d in the Supporting Information) all share the same core and differ only in the design of two (compare A to A^2 and B to B^2) or four (compare A to B and A^2 to B^2) pairs of sticky ends, thus leaving unchanged the total GC content (58%) of the duplex part of the structure. Despite the identical core, changes in sticky ends unexpectedly led to significantly different values of thermal stability, as indicated by a difference of more than 150 kcal mol^{-1} in enthalpy and more than 1 °C in melting temperature (Table 1). Moreover, experiments in which tile A was modified with respect to the number of its sticky ends revealed that the presence/absence and combination of sticky ends can significantly affect the stability and integrity of the tile, even when the core structure remains unchanged (Table S3 and Figure S8 in the Supporting Information). Therefore, these data clearly demonstrate that, even when the duplex core of a tile is held constant, sequence modifications in the nonduplex parts can induce significant variations in the thermal stability of the entire superstructure.

We then investigated the effects of a more drastic design variation, as realized in tile B^3 (Figure S1e in the Supporting Information). Although the total number of base pairs was kept identical to the other tiles, the sequences of all nine oligomers building up tile B^3 were modified, thereby leading to a final GC content of 46% of the duplex core of B^3 (compare 58% for tiles A, A^2, B, and B^2). In spite of its lower GC content, tile B^3 showed a higher thermal stability than tile A but a similar stability to tile B (Table 1).

These results suggest that other factors besides the GC content (such as, for example, the "breathing" of DNA ends, stacking interactions between adjacent bases, hydration effects, and other conformation-dependent forces) play a crucial role in the stability of complex DNA superstructures, whose description as a simple association of stretches of canonical B-DNA duplexes is obviously too restrictive.[9,10]

Finally, we also investigated the assembly of tiles A^2 and B^3 into extended lattices A^2B^3 using two different labeling

strategies (Figure 2 and Figure S7). On the one hand, single tiles, either A^2 or B^3, were labeled as described above; on the other hand, to monitor tile-to-tile assembly into the supramolecular lattice A^2B^3, we chose the opposite termini of the NE and SE oligomers for fluorescence labeling (5′-Fsc-labeled NE strand in tile A^2 and 3′-TAMRA-labeled BSE-3 strand in tile B^3; see Figure 2a). Using the single-tile labeling strategy (Figure 2c, and Figure S7c in the Supporting Information), we could clearly see both the first step of nanoarray assembly, that is, the formation of the single tiles (associated with a T_m value of 59.7 °C and 63.8 °C for tiles A^2 and B^3, respectively), as well as the second step (the tile-to-tile association through their sticky ends, associated with a T_m value of 44 °C). However, this two-transition curve cannot be used for van't Hoff analysis, because this analysis requires a single and reversible transition between only two states. We therefore analyzed the tile-to-tile assembly separately, using the two-tile labeling strategy (Figure 2a), which revealed the expected two-state transition suitable for van't Hoff analysis (Figure 2b and Figure S7a). The respective thermodynamic data indicated weaker thermal stabilities than the single tile formation (Table 1), likely because only sticky-end hybridization between the two tiles is represented by these values. The successful assembly of the A^2B^3 superlattices was also confirmed by the AFM imaging (Figure S3 in the Supporting Information). Additional controls which lacked oligomers AN and BS-3 (A^2B^3(nc) in Table 1 and Figure S7b of the Supporting Information) revealed no thermal transition during the assembly/disassembly process.

In conclusion, the above data clearly indicate the potential of our method to monitor in real time the formation of supramolecular DNA nanostructures. We note that, to the best of our knowledge, no other method has yet been described to provide a full thermodynamic characterization of the self-assembly of DNA nanostructures. Moreover, our method has obvious advantages in terms of time and material consumption. Small quantities (30 μL) of up to 96 samples can be analyzed in parallel to investigate reproducibility and changes in sequence design and experimental conditions, such as oligomer concentration, ionic strengths, and buffer composition. We anticipate that our method is readily applicable to explore and optimize design and experimental parameters of DNA nanostructure formation and thus will contribute to further advances of DNA-based nanotechnology.

Received: October 18, 2007
Revised: December 3, 2007
Published online: February 7, 2008

Keywords: DNA nanostructures · FRET (Förster resonance energy transfer) · nanobiotechnology · self-assembly · thermal analysis

[1] N. C. Seeman, *J. Theor. Biol.* **1982**, *99*, 237–247.
[2] For recent review articles, see: N. C. Seeman, *Nature* **2003**, *421*, 427–431; K. V. Gothelf, T. H. LaBean, *Org. Biomol. Chem.* **2005**, *3*, 4023–4037; U. Feldkamp, C. M. Niemeyer, *Angew. Chem.* **2006**, *118*, 1888–1910; *Angew. Chem. Int. Ed.* **2006**, *45*, 1856–1876; C. Lin, Y. Liu, S. Rinker, H. Yan, *ChemPhysChem* **2006**, *7*, 1641–1647; N. C. Seeman, *Mol. Biotechnol.* **2007**, *37*, 246–257, and references therein.
[3] For general principles of FRET spectroscopy and its application on the study of nucleic acid hybridization, see: T. Förster, *Ann. Phys.* **1948**, *2*, 55–75; L. Stryer, R. P. Haugland, *Proc. Natl. Acad. Sci. USA* **1967**, *58*, 719–726; R. H. Fairclough, C. R. Cantor, *Methods Enzymol.* **1978**, *48*, 347–379; R. M. Clegg, *Methods Enzymol.* **1992**, *211*, 353–388; R. M. Clegg, A. I. Murchie, A. Zechel, D. M. Lilley, *Proc. Natl. Acad. Sci. USA* **1993**, *90*, 2994–2998; R. M. Clegg, A. I. Murchie, D. M. Lilley, *Biophys. J.* **1994**, *66*, 99–109; D. M. Lilley, T. J. Wilson, *Curr. Opin. Chem. Biol.* **2000**, *4*, 507–517, and references therein.
[4] H. Yan, S. H. Park, G. Finkelstein, J. H. Reif, T. H. LaBean, *Science* **2003**, *301*, 1882–1884.
[5] Full details on the sequence design, experimental protocols, van't Hoff analyses, gel electrophoresis, and AFM characterization of tiles and lattices are available in the Supporting Information.
[6] An alternative labeling of the "west" arm led to similar results, thus suggesting that the FRET reporters monitor the stability of the entire superstructure rather than that of the substructure in direct proximity of the fluorophores (see Tables S4 and S2, respectively).
[7] We were unable to detect any increase in the TAMRA emission, most likely as a consequence of quenching effects caused by other nondipolar energy-transfer mechanisms, as previously reported for Fsc–TAMRA FRET systems: M. Torimura, S. Kurata, K. Yamada, T. Yokomaku, Y. Kamagata, T. Kanagawa, R. Kurane, *Anal. Sci.* **2001**, *17*, 155–160; L. Edman, U. Mets, R. Rigler, *Proc. Natl. Acad. Sci. USA* **1996**, *93*, 6710–6715; Y. Jia, A. Sytnik, L. Li, S. Vladimirov, B. S. Cooperman, R. M. Hochstrasser, *Proc. Natl. Acad. Sci. USA* **1997**, *94*, 7932–7936; M. Sauer, K.-T. Han, R. Muller, S. Nord, A. Schulz, S. Seeger, J. Wolfrum, J. Arden-Jacob, G. Deltau, N. J. Marx, C. Zander, K. H. Drexhage, *J. Fluoresc.* **1995**, *5*, 247–261. To compensate for changes in the Fsc fluorescence emission because of temperature effects, controls lacking the TAMRA acceptor were run in parallel (for details, see the Supporting Information).
[8] For van't Hoff analysis of two-state equilibrium systems, see: C. R. Cantor, P. R. Schimmel, *Biophysical Chemistry: Part I–III*, W.H. Freeman, New York, **1980**; K. J. Breslauer, *Methods Mol. Biol.* **1994**, *26*, 347–372; J. L. Mergny, L. Lacroix, *Oligonucleotides* **2003**, *13*, 515–537, and references therein. For details on the calculations carried out in this study, see the Supporting Information.
[9] Only few theoretical models for calculation of the stability of complex DNA superstructures have been reported in the literature. For example, molecular dynamic simulations have been carried out for PX and JX tiles: P. K. Maiti, T. A. Pascal, N. Vaidehi, J. Heo, W. A. Goddard III, *Biophys. J.* **2006**, *90*, 1463–1479; P. K. Maiti, T. A. Pascal, W. A. Goddard III, *J. Nanosci. Nanotechnol.* **2007**, *7*, 1712–1720; for additional examples of theoretical models of supramolecular DNA structures, see: C. Anselmi, G. Bocchinfuso, P. De Santis, M. Savino, A. Scipioni, *Biophys. J.* **2000**, *79*, 601–613; C. Anselmi, P. De Santis, R. Paparcone, M. Savino, A. Scipioni, *Biophys. Chem.* **2002**, *95*, 23–47.
[10] Only very few examples of monitoring the melting profile of DNA tiles by UV spectroscopy have been reported: R. Schulman, E. Winfree, *Proc. Natl. Acad. Sci. USA* **2007**, *104*, 15236–15241, and reference [4]. It was observed that the tiles melt cooperatively at approximately 60 °C, thus being in good agreement with the data reported here.

